Pharmaceutical Research, Vol. 22, No. 8, August 2005 (© 2005)
DOI: 10.1007/s11095-005-5267-7

Research Paper

Structural Characterization of a Recombinant Monoclonal Antibody by Electrospray Time-of-Flight Mass Spectrometry

Lintao Wang,[1] Godfrey Amphlett,[1] John M. Lambert,[1] Walter Blättler,[1] and Wei Zhang[1,2]

Received December 2, 2004, accepted March 23, 2005

Purpose. The aim of this study was to perform structural characterization of a recombinant monoclonal antibody (MAb), huN901, by electrospray time-of-flight mass spectrometry (ESI-TOFMS) using both "top-down" and "bottom-up" approaches.
Methods. In the top-down approach, the molecular masses of the deglycosylated huN901 and the light and heavy chains of the antibody were measured by direct infusion MS and liquid chromatography–mass spectrometry (LC–MS). In the bottom-up approach, trypsin and Asp-N protease were used to digest the separated, reduced and alkylated light and heavy chains followed by LC–MS analysis of the digests.
Results. The primary structure and post-translational modifications of huN901 were characterized by both top-down and bottom-up MS approaches. Modifications of N-terminal pyroglutamate formation, cleavage of C-terminal lysine, glycosylation, and deamidation were identified in the antibody heavy chain by both protein mass measurement and peptide mapping. No modifications were found in the complementarity determining regions (CDRs) of both chains. Both trypsin and Asp-N protease digestion had an average sequence recovery of 97%, and generated complimentary mapping results with complete sequence recovery.
Conclusions. ESI-TOFMS is a superior tool to characterize MAb and other complex protein pharmaceuticals.

KEY WORDS: electrospray time-of-flight mass spectrometry; monoclonal antibody; protein characterization; structural post-translational modifications.

INTRODUCTION

Recombinant monoclonal antibodies (MAb) are becoming increasingly important as effective therapeutic agents. Most therapeutic MAbs originated as murine MAbs and were chimerized or humanized to reduce their immunogenicity in humans (1). Although the general structural features of human immunoglobulins including amino acid sequences and disulfide bond patterns have been known for decades, the structural details of each pharmaceutical MAb need to be determined. Like other protein molecules, MAbs may undergo a series of enzymatic and nonenzymatic reactions during their production and storage process, such as glycosylation, oxidation, deamidation, aggregation, proteolytic cleavage, hydrolysis of peptide bonds, and disulfide bond formation (2,3). Some of these reactions may cause a decrease in or complete loss of their biologic activities.

A range of analytical techniques has been used for the characterization of pharmaceutical MAbs. The most commonly applied methods include various chromatographic methods, polyacrylamide gel and capillary electrophoresis, and mass spectrometry (MS) (4–9). To date, MS has attained a central role in the analysis of biological polymers because of the wealth of structural and molecular information that can be obtained from small amounts of sample. Two approaches are often adopted for protein structural characterization by MS. The first approach is a "top-down" approach, which is the direct measurement of the mass of the intact protein molecules and their subunits. This approach is typically used to test for protein identity or to obtain information on the degree of protein modification. The second approach is a "bottom-up" approach or peptide mapping, where proteins are digested enzymatically or chemically and a peptide mass-fingerprint is obtained. By this means, detailed structural information can be obtained, in particular post-translational modifications and degradation products can be characterized. However, the intrinsic properties of certain quadrupole or magnetic scanning MS instruments used previously made it difficult to characterize large proteins or fragments, including heavy and light chains of MAbs (4). In addition, to obtain unambiguous results, other techniques, such as Edman sequencing and amino acid

[1] ImmunoGen, Inc., Cambridge, Maryland 02139, USA
[2] To whom correspondence should be addressed. (e-mail: wei.zhang@immunogen.com)

ABBREVIATIONS: Asn, asparagine; Asp, aspartate; CDR, complementarity determining region; CHO cells, Chinese hamster ovary cells; ESI-TOFMS, electrospray ionization time-of-flight mass spectrometry; GudHCl, guanidine hydrochloride; HPLC, high-performance liquid chromatography; isoAsp, isoaspartate; LC–MS, liquid chromatography–mass spectrometry; MAb, monoclonal antibody; MW, molecular weight; SEC, size-exclusion chromatography; TFA, trifluoroacetic acid.

analysis, were used in conjunction with MS analyses of most peptides (5,8). Moreover, peptide mapping, although a powerful tool for detailed protein structural characterization, is usually not able to achieve complete sequence recovery even when used together with other analytical tools (5,8).

The recently developed technique of electrospray ionization time-of-flight MS (ESI-TOFMS) is particularly useful for structural characterization of large proteins such as MAbs. The capability of ESI-TOFMS to scan over a large range of mass-to-charge ratios (*m/z*) with near constant sensitivity makes it a powerful tool for direct mass measurement for large, intact proteins or protein assemblies (9–13). Also, the high mass resolution and accuracy, combined with the ease of coupling with high-performance liquid chromatography (HPLC), renders it the method of choice for analyzing complex digestion mixtures of antibodies. In this study, ESI-TOFMS was employed to characterize the structure of a humanized MAb, huN901, using both top-down and bottom-up approaches. HuN901 binds to the CD56 [neural cell adhesion molecule (NCAM)] antigen, which is a potential target for the treatment of small cell lung carcinoma (SCLC) and multiple myeloma (14,15). A maytansinoid conjugate of huN901 is currently in phase I/II clinical trials in patients with SCLC (16).

MATERIALS AND METHODS

Materials

The recombinant huN901 MAb (a humanized IgG_1 kappa immunoglobulin) used in this study was produced in CHO cells and kept at 10 mg/ml in 50 mM potassium phosphate buffer (pH 6.5), containing 50 mM NaCl and 3 mM EDTA. TPCK-treated trypsin was bought from Worthington Biochemical Co. Trifluoroacetic acid (TFA) was from Pierce and HPLC-grade acetonitrile from Burdick & Jackson. All other chemicals and enzymes, unless otherwise stated, were purchased from Sigma. Deionized water (18 Ω) used in this study was produced using a MilliQ water purification system.

HPLC Equipment

Unless otherwise specified, the HPLC system used in this study consisted of a Waters Alliance 2695 separation module equipped with a column heating compartment and a Waters 2478 dual-wavelength UV detector.

Mass Spectrometry

A Waters LCT ESI-TOF mass spectrometer was used for protein molecular mass measurement and peptide mapping. The mass spectrometer was maintained at a routine resolution of about 6000. The source temperature was set at 80°C. The nitrogen gas flow rate and the desolvation temperature were set according to the flow rate. For direct infusion MS at a 5 μl/min flow rate, the desolvation gas flow rate was set to 250–300 L/h at a desolvation temperature of about 150°C. For liquid chromatography–mass spectrometry (LC–MS) at 40 μl/min, the desolvation gas flow rate was increased to 500 L/h and the desolvation temperature to 200°C. The capillary and cone voltages were optimized for maximum sensitivity in each experiment. MS data were acquired and processed using Masslynx 4.0 (Waters). Deconvolution of the protein mass spectra was performed using MaxEnt 1.

ESI-TOFMS Analysis of Deglycosylated huN901

HuN901 deglycosylation was achieved by incubating 20 μl (200 μg) of huN901 solution with 2 μl (14 units) of PNGase F (Sigma, G5166) at 37°C overnight. The deglycosylated huN901 solution was desalted using an Amicon 10-kD molecular weight (MW) cut-off filter (Millipore) and the dilution–concentration method. The desalted huN901 sample was mixed 1:1 (v/v) with acetonitrile containing 0.4% formic acid (concentration of huN901 ~1 mg/ml) and then analyzed by direct infusion ESI-TOFMS at 5 μL/min flow rate. For LC–MS analysis, 50 μg of deglycosylated huN901 was loaded onto a PLRP-S HPLC column (2.1 × 50 mm, 8 μm, 4000 Å, Polymer Laboratories) operating at 60°C with a flow rate of 0.2 ml/min. Protein was eluted from the column using a gradient of acetonitrile containing 0.05% TFA (phase B) in water with 0.05% TFA (phase A). The gradient conditions were as follows: 15% B in 2 min, 15–30% B in 0.5 min, 30–80% B in 5 min, 80–98% B in 1 min, 98–15% B in 1 min, and 15% B in 5 min. The HPLC flow was split 1/5 and the 40 μl/min flow was coupled to ESI-TOFMS.

LCMS Analysis of huN901 Light and Heavy Chain

Deglycosylation of huN901 was performed as described above. Reduction of intact and deglycosylated huN901 was performed at about 1 mg/ml with 50 mM dithiothreitol (DTT) in 50 mM potassium phosphate buffer (pH 6.5) at 37°C over a period of 30 min. Samples of 20 μg of reduced huN901 were chromatographed as described above for deglycosylated N901 except that the gradient conditions were as follows: 5% B in 2 min, 5–30% B in 0.5 min, 30–50% B in 10 min, 50–98% B in 1 min, 98–5% B in 0.5 min, and 5% B in 6 min. The total run time was 20 min. The splitting ratio to MS was 1/5.

Reduction and Alkylation of huN901 for Peptide Mapping

A solution of 200 μl of huN901 (2 mg), 1 ml of denaturing buffer (6 M GudHCl, 1 mM EDTA, 0.5 M Tris buffer, pH 8.3), and 60 μl of 1 M DTT were incubated at 37°C for 1 h. Then 120 μl of 1 M iodoacetic acid in 2 M NaOH was added and the solution was kept at room temperature in the dark for 30 min. Finally, 120 μl of 1 M DTT was added to the mixture to react with the excess amount of iodoacetic acid.

Size-Exclusion Chromatography (SEC)

HuN901 light and heavy chains were separated by HPLC using a Pharmacia Superdex 200 HR SEC column and a mobile phase of 3 M GudHCl at a flow rate of 1 ml/min. The sample loading volume was maximally 700–800 μl to ensure baseline separation. The elution was monitored by UV absorbance at 280 nm and fractions from 9.2–12.2 min

(retention times) for the heavy chain and 12.4–14.5 min (retention times) for the light chain were collected. Collected light and heavy chain fractions were concentrated to about 200–300 μl using an Amicon 10-kDa MW cut-off filtering cup (Millipore) and then exchanged into trypsin or Asp-N digestion buffer using the same HPLC system but with a Pharmacia HR 10/10 fast desalting gel filtration column. The mobile phase was 50 mM Tris-HCl (pH 8.2) containing 1 mM $CaCl_2$ (trypsin digestion buffer) or 100 mM Tris-HCl buffer (pH 8.2) containing 10 mM calcium chloride (Asp-N digestion buffer). The flow rate was 1.5 ml/min, and the chromatography was followed by UV detection at 280 nm. The expected protein component eluted in about 800 μl.

Trypsin Digestion

HuN901 light and heavy chain samples were digested with TPCK-treated trypsin at an enzyme/substrate (E/S) ratio of 1/50 (w/w) in 50 mM Tris-HCl buffer (pH 8.2) containing 1 mM $CaCl_2$ at 37°C overnight. The reaction was quenched by the addition of 30 μl of 1 M HCl to every 1 ml of reaction solution.

Asp-N Protease Digestion

HuN901 light and heavy chain samples were digested with Asp-N protease at an E/S ratio of about 1/100 (w/w) in 100 mM Tris-HCl buffer (pH 8.2) containing 10 mM calcium chloride at 37°C overnight. The reaction was quenched by the addition of 55 μl of 1 M HCl to every 1 ml of digestion solution.

LC–MS Analysis of Tryptic Digests

Tryptic digest samples of huN901 light and heavy chains were separated on a Jupiter Proteo C_{18} column (4.6 × 250 mm, 4 μm, 90 Å, Phenomenex) connected to ESI-TOFMS. The HPLC column was kept at 37°C and eluted at a flow rate of 1.0 ml/min. A T-flow splitter was used to send a flow of 40 μl/min to the ESI-MS probe. Peptides were separated by elution with a gradient of acetonitrile containing 0.05% TFA (phase B) in water with 0.05% TFA (phase A). Gradient conditions were as follows: 0–5 min, 0% B; 5–125 min, 0–40% B; 125–126 min, 40–100% B; 126–134 min, 100% B; 134–135 min, 100–0% B; 135–145 min, 0% B. The HPLC flow of the first 5 min was diverted to waste.

LC–MS Analysis of Asp-N Protease Digests

The Asp-N protease digests of huN901 light and heavy chains were analyzed using a Jupiter C_{18} column (2.1 × 250 mm, 5 μm, 300 Å, Phenomenex) at a flow rate of 0.2 ml/min. The column was set at 35°C and coupled with ESI-TOFMS. A T-flow splitter was used to send a flow of 40 μl/min to the MS probe. Peptides were separated by gradient elution using water as mobile phase A and acetonitrile as mobile phase B, both with 0.1% (w/v) TFA. Gradient conditions were as follows: 0–5 min, 0–5% B; 5–125 min, 5–35% B; 125–130 min, 35–98% B; 130–135 min, 98–98% B; 135–136 min, 98–0% B; 136–145 min, 0% B. The HPLC flow of the first 5 min was diverted to waste.

N-Terminal Sequencing

To confirm sequence assignments by LC–MS, several HPLC fractions of the tryptic and Asp-N protease digests were collected and subjected to Edman sequencing on an Applied Biosystems Model 494 Precise protein sequencer equipped with a Model 140C microgradient delivery system and Model 785A programmable absorbance detector.

MS/MS Analysis

MS/MS analysis of selected HPLC fractions of tryptic and Asp-N protease digests was performed using a Bruker Esquire ion-trap or a Waters QTOF-API-US mass spectrometer to confirm sequence assignments from LC–MS results. Samples were infused without pre-concentration at 5 μl/min and standard ESI parameters were used. Collision energy was optimized for optimum signal-to-noise ratios of fragment ions.

RESULTS

Analysis of huN901 Antibody by a Top-Down MS Approach

Analysis of huN901 by the top-down approach aims at providing direct information about the molecular mass of the antibody and possible major post-translational modifications. The analysis was performed with deglycosylated huN901 and ESI-TOFMS, which gave a spectrum (Fig. 1A) that consisted of a typical series of multiply charged species with the *m/z* values ranging from 2000 to about 4000. The corresponding

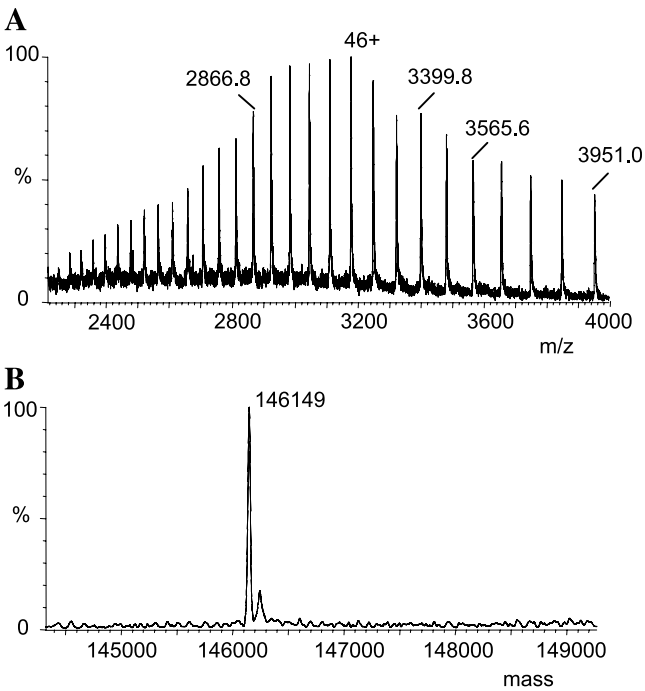

Fig. 1. ESI-TOFMS spectra of deglycosylated huN901 obtained by LCMS analysis. (A) MS raw data showing a series of multiply charged molecular ions. (B) Deconvoluted MS spectra showing the molecular mass of the antibody. The minor peak in (B) is due to unknown salt adduction.

deconvoluted spectrum is shown in Fig. 1B and shows a measured mass of 146,149 Da. The error range for the mass measurement was within 0.01%, given careful mass calibration and minimal temperature fluctuations.

Based on the cDNA-derived amino acid sequence of huN901 (Fig. 2), the heavy and light chains have a calculated molecular mass of 49,121 Da and 24,113 Da, respectively, which yields a calculated mass for the whole MAb of 146,436 Da with the 16 disulfide bonds expected for an IgG_1-type MAb taken into consideration. This differs from the measured mass by 287 Da, indicating that the protein underwent post-translational modifications in addition to disulfide bond formation. Potential modifications in the heavy chain include the cleavage of the C-terminal lysine and conversion of the N-terminal glutamine to pyroglutamic acid (6,13,19), which would cause a mass decrease by two times 128 Da and two times 17 Da, respectively. In addition, deglycosylation in both heavy chains changes Asn to Asp and increases the mass by 2 Da. Based on these modifications, the calculated molecular mass of deglycosylated huN901 is 146,148 Da, which differs by only 1 Da from the measured value. The closeness of this calculated mass to the experimental mass (well within experimental error of +/− 0.01%) suggests that huN901 underwent these modifications in both heavy chains. No additional modifications in the light chain are necessary to explain the measured molecular mass.

Analysis of huN901 light and heavy chains provided further experimental evidence for these post-translational modifications. Both intact and deglycosylated huN901 were reduced and their light and heavy chains analyzed by LC–MS. The ESI–MS spectra are presented in Fig. 3. The measured mass of the deglycosylated light chain was 24,109 Da, which is 4 Da lower than the calculated value (24,113 Da), whereas that of the deglycosylated heavy chain was found to be 48,967 Da, which is 10 Da lower than the calculated value (48,977 Da) for a heavy chain that had undergone the three post-translational modifications discussed earlier. These mass discrepancies are outside the error range (+/− 0.01%) of the MS instrument. We speculated that they might be the result of incomplete disulfide bond reduction caused by the mild reduction conditions used (pH 6.5 without denaturant). Alkylation experiments of light and heavy chains reduced at same conditions supported our interpretation of incomplete reduction (data not shown). Assuming that only the interchain disulfide bonds are reduced while the intrachain bonds remain intact, the calculated molecular masses of the huN901 light and deglycosylated heavy chains are 24,109 Da and 48,969 Da, respectively, which would be

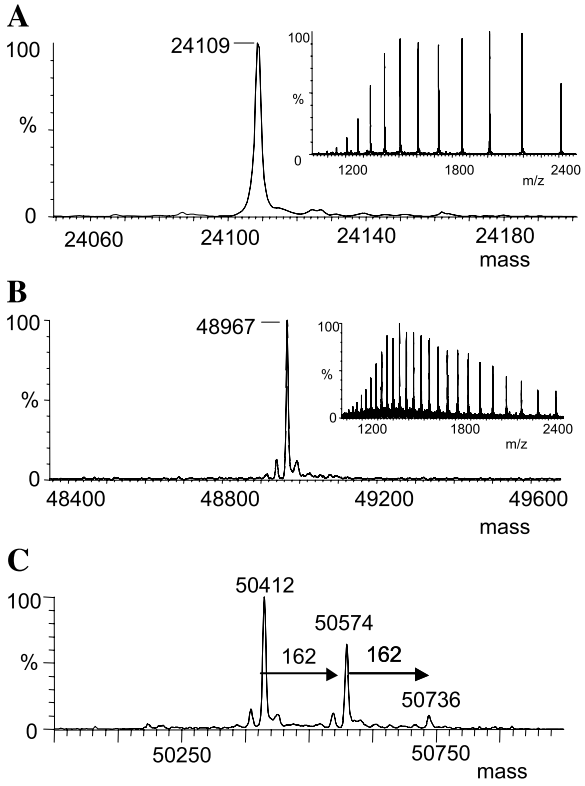

Fig. 3. ESI-TOFMS spectra of huN901 light chain (A), deglycosylated heavy chain (B), and glycosylated heavy chain (C). The inserts in A and B show the raw MS spectra. The minor peaks on both sides of the peaks of 48,967 Da in (B) and 50,412 Da and 50,574 Da in (C) are artifacts from deconvolution.

A

DVVMTQSPLS LPVTLGQPAS ISC**RSSQIII HSDGNTYLE**W FQQRPGQSPR 50
RLIY**KVSNRF S**GVPDRFSGS GSGTDFTLKI SRVEAEDVGV YYC**FQGSHVP** 100
HTFGQGTKVE IKRTVAAPSV FIFPPSDEQL KSGTASVVCL LNNFYPREAK 150
VQWKVDNALQ SGNSQESVTE QDSKDSTYSL SSTLTLSKAD YEKHKVYACE 200
VTHQGLSSPV TKSFNRGEC 219

B

<QVQLVESGGG VVQPGRSLRL SCAASGFTFS **SFGMH**WVRQA PGKGLEWVA**Y** 50
ISSGSFTIYY ADSVKGRFTI SRDNSKNTLY LQMNSLRAED TAVYYCAR**MR** 100
KGYAMD**Y**WGQ GTLVTVSSAS TKGPSVFPLA PSSKSTSGGT AALGCLVKDY 150
FPEPVTVSWN SGALTSGVHT FPAVLQSSGL YSLSSVVTVP SSSLGTQTYI 200
CNVNHKPSNT KVDKKVEPKS CDKTHTCPPC PAPELLGGPS VFLFPPKPKD 250
TLMISRTPEV TCVVVDVSHE DPEVKFNWYV DGVEVHNAKT KPREEQY▲ST 300
YRVVSVLTVL HQDWLNGKEY KCKVSNKALP APIEKTISKA KGQPREPQVY 350
TLPPSRDELT KNQVSLTCLV KGFYPSDIAV EWESNGQPEN NYKTTPPVLD 400
SGDSFFLYSK LTVDKSRWQQ GNVFSCSVMH EALHNHYTQK SLSLSPG 447

Fig. 2. The amino acid sequence of huN901 light chain (A) and heavy chain (B). The heavy chain was labeled with the following post-translational modifications: N-terminal pyro-glutamine (<Q), N-glycosylation (▲ below Asn298), and loss of the C-terminal Lys. Residues in bold are CDRs. Residues not detected in the trypsin or Asp-N protease digestion are underlined by solid and dotted lines, respectively.

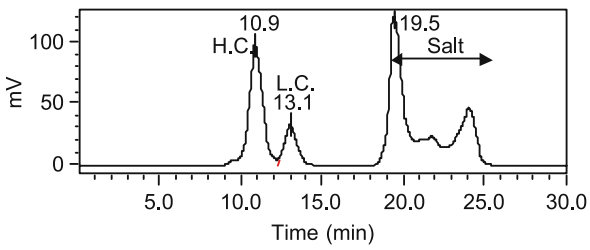

Fig. 4. Size-exclusion chromatogram of reduced and alkylated huN901 light chain (L.C.) and heavy chain (H.C.) in 3 M GudHCl (UV absorbance at 280 nm).

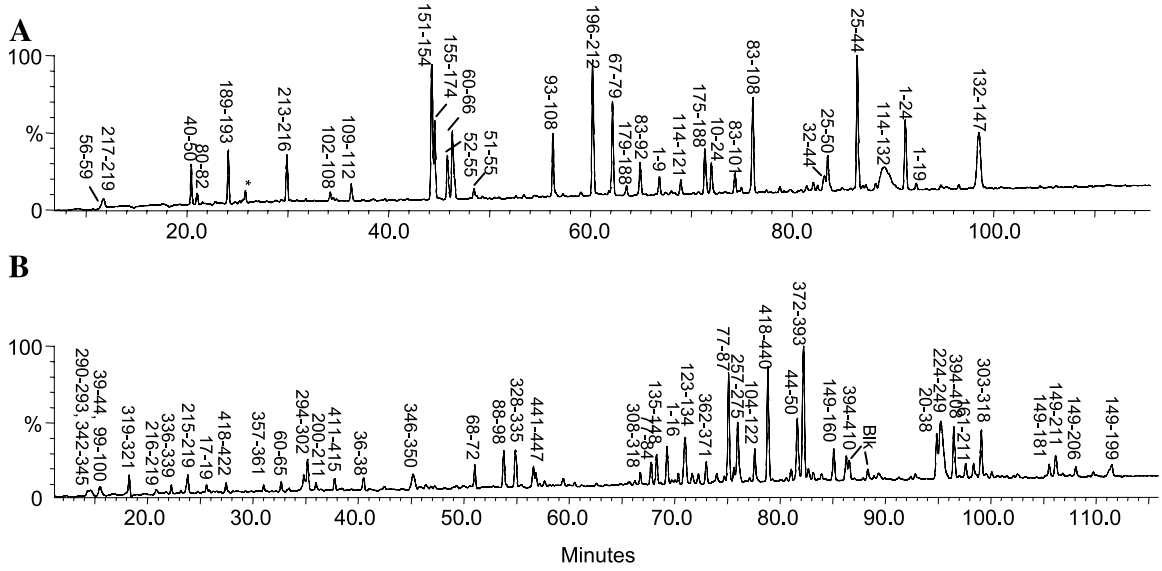

Fig. 5. HPLC UV chromatograms of LCMS analysis of tryptic digests of huN901 light chain (A) and heavy chain (B) labeled with peptide sequences. Peaks present in the blank control are labeled with "Blk." Unidentified peaks are labeled with stars.

Table I. Tryptic Peptides of huN901 Light Chain

Peptide	Re. time (min)	Area %	From–to	Sequence	Exp. mass (Da)	Cal. mass (Da)	Error (Da)
T1	91.2	65	1–24	DVVMT..SBR	2556.14	2556.29	−0.15
T1′a	66.8	13	1–9	DVV..SPL	988.42	988.49	−0.07
T1′b	72.0	25	10–24	(L)SLP..SBR	1585.72	1585.81	−0.09
T1′c	92.3	6	1–19	DVV..PA(S)	1951.96	1952.03	−0.07
T2	83.5	25	25–50	(R)SSQ..SPR	3043.29	3043.49	−0.20
T2′a	20.4	22	45–50	(R)PGQSPR	640.30	640.33	−0.03
T2′b	52.6	5	25–31	(R)SS...IH	796.38	796.44	−0.06
T2′c	83.2	13	32–44	(H)SD..QQR	1642.64	1642.74	−0.10
T2′d	86.5	100	25–44	(R)SSQ..QQR(P)	2421.04	2421.17	−0.13
T3T4	48.5	5	51–55	(R)RLIYK	691.40	691.44	−0.04
T4	45.8	31	52–55	(R)LIYK	535.30	535.34	−0.04
T5	11.7	13	56–59	(K)VSNR	474.21	474.26	−0.05
T6	46.3	49	60–66	(R)FSGVPDR	776.30	776.38	−0.08
T7	62.2	67	67–79	(R)FSG...TLK	1302.50	1302.61	−0.11
T8	21.0	7	80–82	(K)ISR	374.20	374.23	−0.03
T9′a	34.2	5	102–108	(H)TFGQGTK	737.30	737.37	−0.07
T9′b	46.5	9	95–108	(F)QGS..GTK	1479.60	1479.72	−0.12
T9′c	56.3	39	93–108	(Y)BTQ..GTK	1787.60	1787.80	−0.20
T9′d	64.9	23	83–92	(R)VEA..VYY	1142.44	1142.51	−0.07
T9′f	74.3	14	83–101	(R)VEA..PH(T)	2192.80	2192.95	−0.15
T9	76.1	69	83–108	(R)VEA...GTK	2912.22	2912.31	−0.09
T10	36.3	11	109–112	(K)VEIK	487.30	487.30	0.00
T12′	69.0	13	114–121	(R)TVAAPSVF	790.38	790.42	−0.04
T12	89.2	77	114–132	(R)TVAA..SDEQLK	1944.88	1945.02	−0.14
T13	98.5	100	132–147	(K)SGTA..NNFYPR	1797.76	1797.87	−0.11
T15	44.3	100	151–154	(K)VQWK	559.30	559.31	−0.01
T16	44.6	50	155–174	(K)VDN..GNS..DSK	2134.802	2134.96	−0.16
T17′	63.6	8	179–188	(Y)SLSS..LSK	1035.51	1035.58	−0.07
T17	71.4	35	175–188	(K)DSTY..LSK	1501.64	1501.75	−0.11
T18	24.1	33	189–193	(K)ADYEK	642.20	624.28	−0.08
T20	60.2	94	196–212	(K)VYAB...VTK	1875.76	1875.90	−0.14
T21	29.9	29	213–216	(K)SFNR	522.20	522.26	−0.06
T22	11.7	2	217–219	(R)GEB	365.05	365.09	−0.04

[a]Tn′ or Dn′ indicates partial sequence of tryptic peptide Tn or Asp-N protease peptide Dn;
[b]X, B and O in peptide sequences represent pyroglutamic acid, carboxymethylated cysteine and N-glycosylated asparagine, respectively;
[c]Residues next to the identified peptide are shown in parentheses;
[d]dN = deamidation;
[e]Peak areas are normalized to the largest peak area in the UV chromatogram.

Table II. Tryptic Peptides of huN901 Heavy Chain

Peptide	Re. time (min)	Area %	From–to	Sequence	Exp. mass (Da)	Cal. mass (Da)	Error (Da)
T1	69.3	24	1–16	(−)XQVQLV..VQPGR	1591.78	1591.83	−0.05
T2	25.6	4	17–19	(R)SLR	374.22	374.23	−0.01
T3	94.9	33	20–38	(R)LSBA..MHWVR	2147.90	2147.96	−0.06
T3′	40.5	10	36–38	(H)WVR	459.25	459.26	−0.02
T4	15.5		39–44	(R)QAPGK	499.28	499.28	0.00
T5′a	32.7	6	60–65	(Y)YADSVK	681.34	681.33	0.01
T5′b	75.6	8	51–65	(Y)ISSG..DSVK	1636.78	1636.80	−0.02
T5′c	81.7	51	44–50	(K)GLE..TIY	836.40	836.41	−0.01
T5	106.5		44–65	(K)GLEWV..ADSVK	2455.20	2455.19	0.01
T7	51.0	13	68–72	(R)FTISR	622.34	622.34	0.00
T9′	67.8	15	77–84	(K)NTLYQMN	995.47	995.47	0.00
T9	75.1		77–87	(K)NTLYLQMNSLR	1351.70	1351.69	0.01
T10	53.8	26	88–98	(R)AEDTAVYYBAR	1318.51	1318.55	−0.04
T11	15.5		99–10	(R)MR	305.15	305.15	0.00
T13′	77.6	23	104–122	(Y)AMDYWGQ..ASTK	2000.92	2000.95	−0.03
T13	82.2		102–122	(K)GYAMD..ASTK	2221.00	2221.04	−0.04
T14	71.0	39	123–134	(K)GPSVFPLAPSSK	1185.62	1185.64	−0.02
T15	68.3	20	135–148	(K)STSGGTAA.LVK	1321.62	1321.65	−0.03
T16′a	36.0	3	200–211	(Y)IBNV...NTK	1411.64	1411.69	−0.05
T16′b	85.1	24	149–160	(K)DYFPEPVTVSWN	1452.62	1452.66	−0.04
T16′c	97.6	11	161–211	(N)SGAL...NTK	5282.08	5281.89	0.19
T16′d	105.5	8	149–181	(K)DYFPEP..SSGLY(S)	3525.74	3525.70	0.04
T16′f	108.1	8	149–206	(K)DYF..NHK(P)	6190.00	6189.87	0.13
T16′g	111.5	10	149–199	(K)DYFP..GTQTY	5322.90	5322.87	0.03
T16	106.2	16	149–211	(K)DYFP..NVNHKPSNTK	6717.72	6717.44	0.28
T18T19	23.8	13	215–219	(K)KVEPK	599.35	599.36	−0.01
T19	20.8	4	216–219	(K)VEPK	471.28	471.27	0.01
T20	6.6	2	220–223	(K)SBDK	509.17	509.18	−0.01
T20	8.7	2	220–223	(K)SBDK	509.17	509.18	−0.01
T21	95.3	80	224–249	(K)THTBPPB..PPKPK	2845.35	2845.42	−0.07
T21′	89.4	6	224–242	(K)THT..SVF	2037.88	2037.92	−0.04
T22	56.9	9	250–256	(K)DTLMISR	834.40	834.43	−0.03
T23	76.0	40	257–275	(R)TPEV..DPEVK	2138.96	2139.00	−0.04
T24	75.1	73	276–289	(K)FNWY..HNAK	1676.76	1676.79	−0.03
T24′	78.9		276–286	(K)FNWYVDGVEVH	1363.62	1363.62	0.00
T25	14.3	4	290–293	(K)TKPR	500.27	500.31	−0.04
T26(G0)	35.2	23	294–302	(R)EEQ...TYR(+glycan)	2633.00	2633.04	−0.04
T26(G1)	34.7	12	294–302	(R)EEQ...TYR(+glycan)	2794.96	2795.09	0.13
T27′	66.7	8	308–318	(L)TVLHQDWLNGK	1309.66	1309.68	−0.02
T27	99.1	35	303–318	(R)VVS..LNGK	1807.00	1807.00	0.00
T27dN	98.4	9	303–318	(R)VVS..LNGK (dN)	1808.00	1808.00	0.00
T28	18.3	18	319–321	(K)EYK	438.21	438.21	0.00
T30	5.7	2	324–327	(K)VSNK	446.23	446.25	−0.02
T31	54.9	27	328–335	(K)ALPAPIEK	837.50	837.50	0.00
T32	22.3	5	336–339	(K)TISK	447.27	447.27	0.00
T34	14.6	7	342–345	(K)GQPR	456.24	456.24	0.00
T35′	45.2	20	346–350	(R)EPQVY	634.29	634.30	−0.01
T36	31.0	4	357–361	(R)DELTK	604.29	604.31	−0.02
T37	73.0	13	362–371	(K)NQVSLTBLVK	1161.57	1161.61	−0.04
T38	82.2	100	372–393	(K)GFYP..NG..PENNYK	2543.06	2543.12	−0.06
T39′	96.5		394–408	(K)TTPP...FLY	1657.74	1657.79	−0.05
T39′	96.5		398–410	(P)VLD..YSK	1476.70	1476.71	−0.01
T39	86.3	17	394–410	(K)TTPPV..FLVSK	1872.88	1872.91	−0.03
T40	37.8	6	411–415	(K)LTVDK	574.31	574.33	−0.02
T42	78.9	78	418–440	(R)WQQGN..NHYTQK	2801.19	2801.24	−0.05
T43	56.6	15	441–447	(K)SLSLSPG	659.34	659.35	−0.01

[a] Tn′ or Dn′ indicates partial sequence of tryptic peptide Tn or Asp-N protease peptide Dn;
[b] X, B and O in peptide sequences represent pyroglutamic acid, carboxymethylated cysteine and N-glycosylated asparagine, respectively;
[c] Residues next to the identified peptide are shown in parentheses;
[d] dN = deamidation;
[e] Peak areas are normalized to the largest peak area in the UV chromatogram.

consistent with the experimental values. More complete reduction of both chains of huN901 was achieved in the presence of 5 M GudHCl at pH 8.3, which was indicated by mass increases of 4 Da and 8 Da for light and heavy chains, respectively (data not shown). However, the MS spectra, particularly that of the heavy chain, had a low signal-to-noise ratio, possibly as a result of protein aggregation during sample preparation and analysis.

The LC–MS analysis of the reduced huN901 indicated glycosylation in the heavy chain. The ESI-MS spectrum of the glycosylated heavy chain (Fig. 3C) shows three peaks spaced equally with a mass difference of 162 Da, suggesting the presence of three types of oligosaccharide chains that differ from each other by one and two hexose units. Oligosaccharides in the heavy chain of recombinant huIgG$_1$ are typically N-linked to an Asn of an Asn-X-Thr/Ser sequence and share a bi-antennary, fucosylated core (17–19). The core structure may be attached with 0, 1, or 2 terminal galactosyl, which are named G0, G1, and G2, respectively. The lowest mass of the three peaks in huN901 heavy chain spectrum (50,412 Da; Fig. 3C) was 1,445 Da higher than the mass of the deglycosylated heavy chain (48,967 Da; Fig. 3B). This mass difference matches with the fucosylated bi-antennary structure with no galactosyl residue (G0). By calculation, the peaks with masses 162 Da and 324 Da larger than that of G0 correspond to the G1 and G2 species, respectively. Other glycan forms, for example, glycans with sialic acid, were not observed.

To further confirm the above post-translational modifications in huN901 and determine their locations in the amino acid sequence, we analyzed huN901 with the bottom-up approach of peptide mapping by LC–MS. This approach also has the advantage of detecting modifications of relatively lower abundance or modifications with small mass differences such as deamidation. Both trypsin and Asp-N protease were used to obtain complementary results and to increase the overall sequence recovery. To reduce the complexity and therefore enhance the separability of the enzymatic digestion mixtures, we performed denaturing size-exclusion chromatography (SEC) to first separate reduced and alkylated light and heavy chains (Fig. 4) before digesting them with the two enzymes.

Analysis of Trypsin Digests of huN901 Light and Heavy Chains

Complete tryptic digestion of huN901 light and heavy chains was obtained, as evidenced by a lack of protein signal in the washing step by both UV and MS detection. The annotated UV chromatograms of the LC–MS analysis are presented in Fig. 5. The HPLC peaks were assigned a peptide sequence by matching the measured mass of the peptide with the calculated mass of peptides derived from trypsin digestion simulation (T1–T22 for light chain in Table I; T1–T43 for heavy chain in Table II). Some peaks were found to be derived from chymotrypsin-like cleavage, such as the light chain peptides 83–92 and 93–108 (Table I), which was confirmed by CID MS/MS and N-terminal sequencing. For both chains, peptides were identified covering 97–98% of the sequences. Only a few small, hydrophilic peptides, such as residues 148–150 and 194–195 of light chain, were not detected, probably owing to early elution with buffer components. Representative ESI–MS spectra of huN901 tryptic peptides are shown in Fig. 6, which include peptides in CDRs (complementarity determining regions), N-terminal and C-terminal peptides of heavy chain, and glycosylated peptides.

The close match between experimental and calculated masses of huN901 CDR peptides indicated no post-translational modifications in the CDRs (Fig. 6A, B; Tables I and II). Several modifications including those identified by the top-down approach were observed in the heavy chain tryptic mapping. The heavy chain peptide with N-terminal pyroglutamic acid (HT1, residues 1–6, Fig. 6C) was found eluting at 69.3 min (Fig. 5B). The heavy chain C-terminal peptide lacking the terminal lysine residue (HT43, residues 441–447, Fig. 6D) was found eluting at 56.6 min (Fig. 5B). Glycosyl-

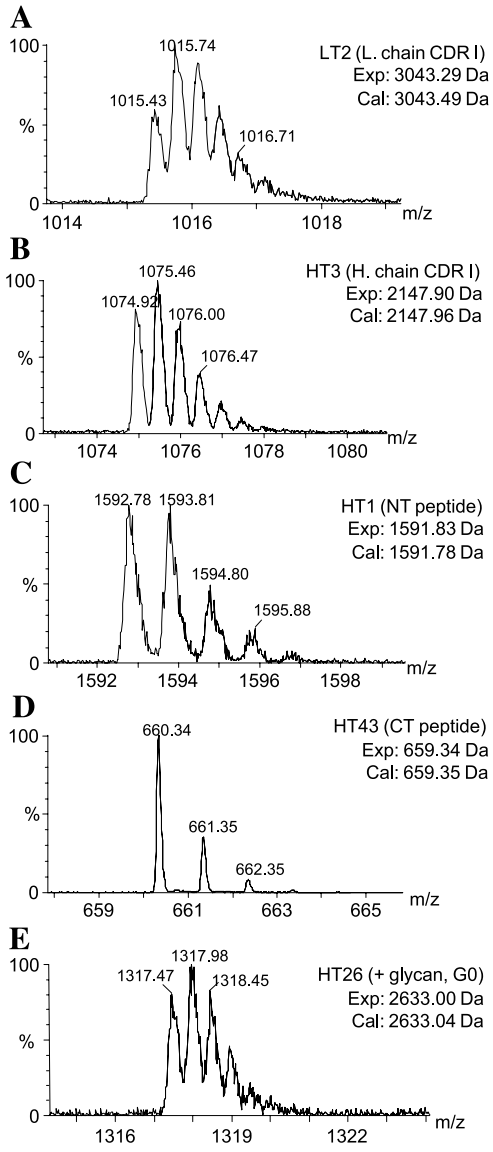

Fig. 6. Representative MS spectra of huN901 tryptic peptides with their experimental and calculated masses. (A) CDR-containing light chain tryptic peptide LT2 (25–50). (B) Heavy chain CDR peptide HT3 (20–38). (C) Heavy chain N-terminal peptide HT1 (1–16). (D) Heavy chain C-terminal peptide HT43 (441–447). (E) Glycosylated peptide HT26 (294–302, G0).

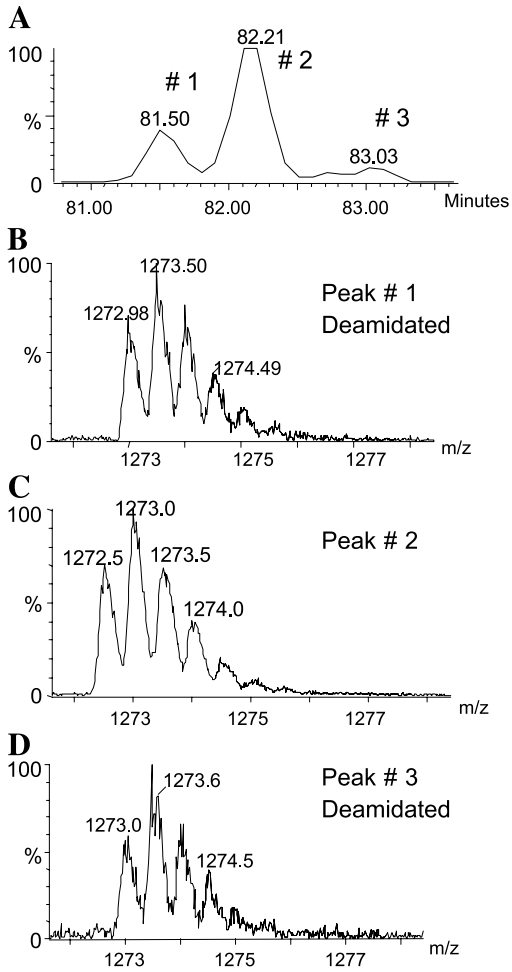

Fig. 7. Enlarged extracted ion chromatogram (*m/z* 1272–1275, A) and MS spectra of huN901 heavy chain tryptic peptide HT38 (C) and its deamidated products (B, D).

ation of huN901 heavy chain was confirmed by finding glycosylated peptides eluting in the range from 34.7–35.2 min (Fig. 5B). MS analysis gave several molecular masses corresponding to the peptide HT26 (residues 294–302) linked to one of the three oligosaccharides (G0, G1, and G2) as described earlier. The MS spectrum of the peptide linked to G0 is shown in Fig. 6E. Asn298 is the only potential N-linked glycosylation site in this peptide and thus is determined to be the N-glycosylation site.

Deamidations of Asn residues were also detected by tryptic digestion of huN901. Two heavy chain peptides, HT27 (303–318) and HT38 (372–393), were found in both their native and their deamidated forms, as indicated by the existence of neighboring HPLC peaks with masses increasing by 1 Da (i.e., peak at 98.4 min for HT27 in Table II, and peaks 1 and 3 in Fig. 7). In HT27, Asn316, the only Asn residue with the subsequence of Asn-Gly, is likely the deamidation site. The Asn residue with the subsequence of Asn-Gly has been reported to be deamidated in other recombinant antibodies as well (8,20). In HT38, there are three Asn residues and two peaks have been observed with 1-Da mass increase (i.e., peaks 1 and 3 in Fig. 7). MS/MS analysis of peak 1 of Fig. 7 indicated deamidation at the residue Asn385 in the subsequence Asn-Gly (Fig. 8). MS/MS analysis of peak 3 of Fig. 7 gave somewhat different spectrum from that in Fig. 8. The *m/z* ratios of fragment ions y6 and y4 were observed to be 765 and 539 instead of 764 and 538, respectively, while y3 remained same (spectrum not shown), which indicated that Asn390 was deamidated in peak 3. The deamidation of Asn in proteins and peptides is believed to proceed via a succinimide intermediate followed by hydrolysis into isoaspartate or aspartate (2,21,23). Asp-N digestion may distinguish between Asp and isoAsp containing species since Asp-N protease cannot cleave at isoAsp residues (21).

Analysis of Asp-N Protease Digests of huN901 Light and Heavy Chains

The UV chromatograms of the LC–MS analysis of Asp-N protease digests of huN901 light and heavy chain are presented in Fig. 9. Similar to trypsin digestion, no undigested protein was found by UV or MS detection, even in the column washing step. The HPLC peak assignments were made according to peptide mass measurement, MS/MS, and

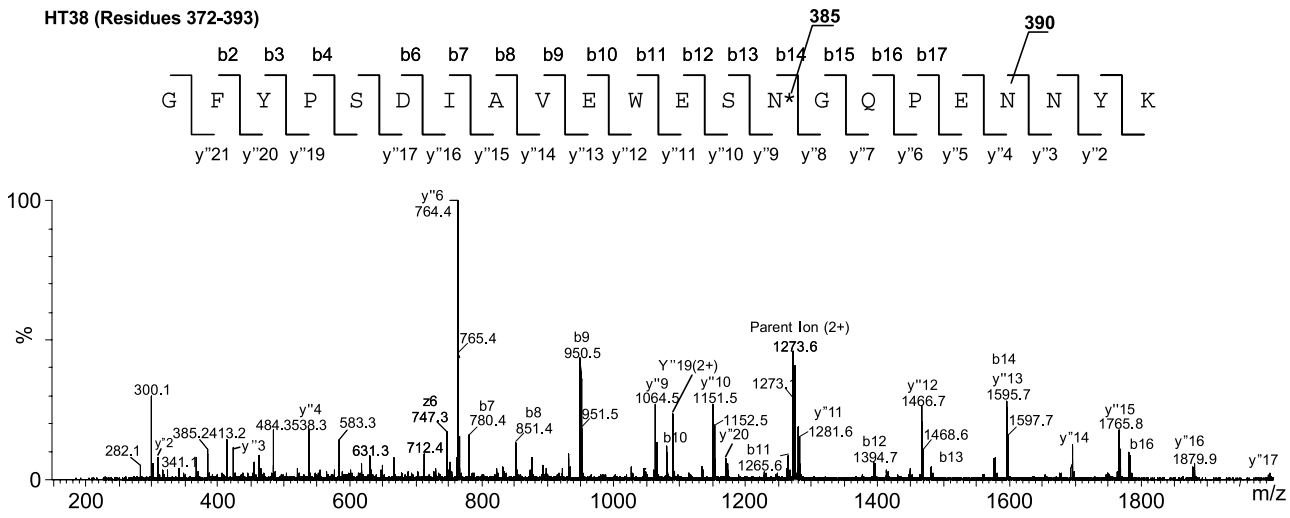

Fig. 8. MS/MS spectrum of huN901 heavy chain tryptic peptide HT38 that had undergone deamidation (peak 1 in Fig. 7). The deamidated Asn residue is indicated by N* in the peptide sequence. This analysis was performed using the QTOF mass spectrometer.

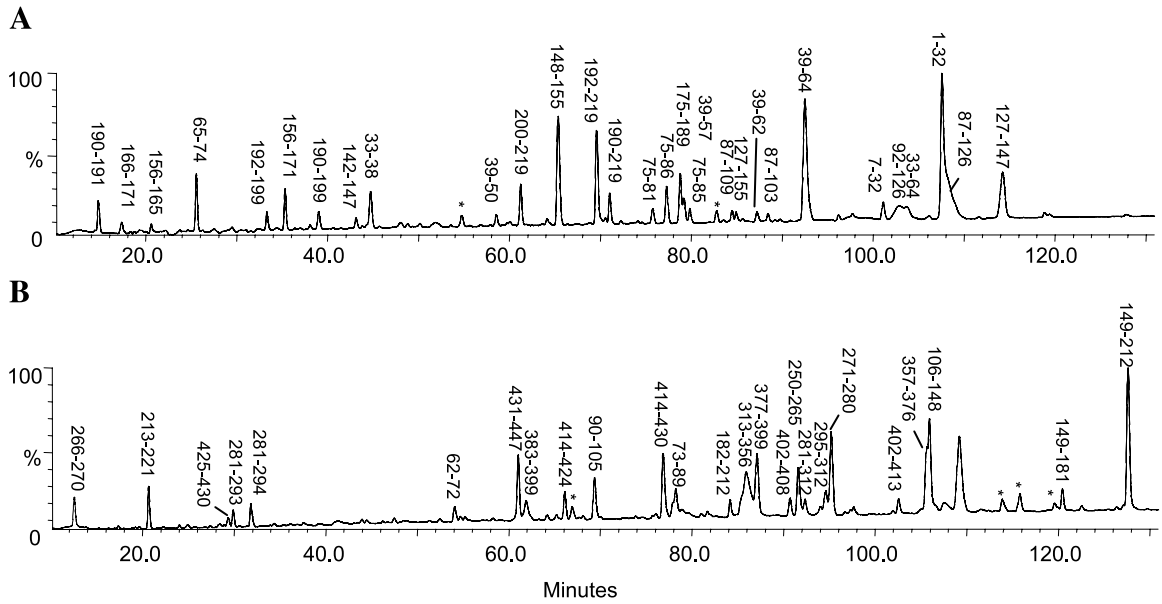

Fig. 9. HPLC UV chromatograms of Asp-N protease digest of huN901 light chain (A) and heavy chain (B). Unidentified peaks are labeled with stars.

N-terminal sequencing. Identified peptides of Asp-N digestion of the light and heavy chains are listed in Tables III and IV, respectively.

Simulation of the Asp-N protease digestion of huN901 gives 10 peptides (D1–D10) for the light chain and 18 peptides (D1–D18) for the heavy chain, most of which were identified in the LC–MS analysis (Tables III and IV). Peptides were also found derived from cleavages at the N-terminal side of glutamic acid and, less frequently, serine. These extra cleavages seemed to be the reason for weak intensities or absence of a few Asp-N peptides. For example, the C-terminal peptide of the heavy chain (HD18; residues 414–447) was not found because of extra cleavages at the N-terminus of Glu431 and Ser425, resulting in smaller peptides composed of residues 414–424, 414–430, and 431–447 (Table IV). MS/MS analysis and N-terminal sequencing were

Table III. Asp-N Peptides of huN901 Light Chain

Peptide	Re. time (min)	Area %	From–to	Sequence	Exp. mass (Da)	Cal. mass (Da)	Error (Da)
D1	107.6		1–32	(−)DVVMTQ..IIIHS(D)	3421.65	3421.76	−0.11
D1′	101.1	10	7–32	(Q)SPSLS..IIIHS(D)	2748.42	2748.45	−0.03
D2	103.7	14	33–64	DGNTY..NRFSGVP(D)	3794.82	3794.94	−0.12
D2′a	44.7	22	33–38	DGNTYL(E)	681.28	681.30	−0.02
D2′b	92.5	100	39–64	EWFQQR..FSGVP(D)	3131.58	3131.65	−0.07
D3	25.5	25	65–74	DRFSGSGSGT(D)	969.38	969.42	−0.04
D4′a	75.8	8	75–81	DFTLKIS	822.44	822.45	−0.01
D4′b	79.8	6	75–85	DFTLKISRVEA(E)	1277.70	1277.70	0.00
D4	77.3	19	75–86	DFTLKISRVEAAE(D)	1406.72	1406.74	−0.02
D5	107.6		87–126	DVGVYY..IFPPS(D)	4425.96	4426.04	−0.08
D5′a	84.5	5	87–109	DVGVYY..QGTKV	2583.15	2583.19	−0.04
D5′b	102.8	13	92–126	(Y) YBFQGS..FIFPPS(D)	3892.32	3892.45	−0.13
D6′a	65.3	64	148–155	EAKVQWKV(D)	986.54	986.55	−0.01
D6′a	114.2	46	127–147	DEQLK..LLNNFYPR(E)	2411.10	2411.18	−0.08
D7	35.3	18	156–171	DNALQSGNSQESVTEQ	1705.66	1705.74	−0.08
D9	78.8	29	175–189	DSTYS..TLSKA(D)	1572.76	1572.79	−0.03
D10′a	14.8	14	190–191	DY(E)	296.12	296.10	0.02
D10′b	33.3	9	192–199	EKHKVYAB (E)	1034.46	1034.48	−0.02
D10′c	61.2	21	200–219	EVTHQ..FNRGEB(−)	2232.99	2233.04	−0.05
D10′d	69.6	44	192–219	EKHKV..FNRGEB(−)	3249.39	3249.52	−0.13
D10	71.0	14	190–219	DYEKH..FNRGEB(−)	3527.49	3527.61	−0.12

[a] Tn′ or Dn′ indicates partial sequence of tryptic peptide Tn or Asp-N protease peptide Dn;
[b] X, B and O in peptide sequences represent pyroglutamic acid, carboxymethylated cysteine and N-glycosylated asparagine, respectively;
[c] Residues next to the identified peptide are shown in parentheses;
[d] dN = deamidation;
[e] Peak areas are normalized to the largest peak area in the UV chromatogram.

Table IV. Asp-N Peptides of huN901 Heavy Chain

Peptide	Re. time (min)	Area %	From–to	Sequence	Exp. mass (Da)	Cal. mass (Da)	Error (Da)
D1	133.2	67	1–61	(−)XVQL..GMH..TIYYA(D)	6571.52	6571.42	0.10
D2	54.1	9	62–72	DSVKGRFTISR(D)	1264.70	1264.69	0.01
D3	78.0	6	73–89	DNSKN..MNSLRAE(D)	1995.96	1995.97	−0.01
D4	69.3	30	90–105	DTAV..MRKGYAM(D)	1955.86	1955.87	−0.01
D5	105.9	69	106–148	DYWG..GBLVK(D)	4272.69	4274.80	−0.11
D6′a	120.5	5	149–181	DYFP..GLY(S)	3525.66	3525.71	−0.05
D6′b	84.2	10	182–212	(Y) SLS..NVN..NTKV(D)	3304.71	3304.66	0.05
D6	127.6	100	149–212	DYFP..NSG..NVNHKPSNTKV(D)	6816.72	6816.58	0.14
D7	20.7	21	213–221	DKKVEPKSB(D)	1090.56	1090.53	0.03
D8	109.2	92	222–249	DKTHTBPPB..PPKPK(D)	3088.50	3088.54	−0.04
D9	91.6	34	250–265	DTLM..BVV(D)	1819.88	1819.91	−0.03
D10	12.5	14	266–270	DVSHEV(D)	585.25	585.24	0.01
D11	95.2	70	271–280	DPEVKFNWYV(D)	1295.64	1295.62	0.02
D12′a	29.9	9	281–293	DGVEVHNAKTKPR(E)	1449.78	1449.77	0.01
D12′b	31.8	13	281–294	DGVE..TKPRE(E)	1578.82	1578.81	0.01
D12′c, G0	94.6	19	295–312	(E)EQYO..VLHQ(D) + Glycan	3579.57	3579.63	−0.06
D12′c, G1	94.0	6	295–312	(E)EQYO..VLHQ(D) + Glycan	3741.63	3741.68	−0.05
D12, G0	92.3	8	281–312	DGV..QYO..HQ(D) + Glycan	5143.48	5143.46	0.02
D13	85.9	75	313–356	DWLNG..NK..PPSR(D)	5025.92	5025.81	0.11
D13, dN	85.5	13	313–356	DWLNG..NK..PPSR(D)	5026.80	5026.81	−0.01
D14	105.7	33	357–376	DEL..NQ..FYPS(D)	2299.12	2299.14	−0.02
D15′a	78.2	23	377–382	DIAVEW(E)	731.35	731.35	0.00
D15′b	61.9	18	383–399	ESNGQPENNY..VL(D)	1886.90	1886.90	0.00
D15	87.1	54	377–399	DIA..SNGQPENNY..VL(D)	2600.18	2600.24	−0.06
D17	102.6	10	402–413	DGSFFLYSKLTV(D)	1375.72	1375.70	0.02
D17′	90.7	14	402–408	DGSFFLY(S)	847.38	847.38	0.00
D18′ a	66.1	20	414–424	DKSR..GNVF(S)	1363.70	1363.66	0.04
D18′b	76.9	46	414–430	DKS..VFSBSVMH(E)	2065.86	2065.91	−0.05
D18′ c	61.0	41	431–447	EALHNH..LSPG(−)	1880.92	1880.94	−0.02

[a] Tn′ or Dn′ indicates partial sequence of tryptic peptide Tn or Asp-N protease peptide Dn;
[b] X, B and O in peptide sequences represent pyroglutamic acid, carboxymethylated cysteine and N-glycosylated asparagine, respectively;
[c] Residues next to the identified peptide are shown in parentheses;
[d] dN = deamidation;
[e] Peak areas are normalized to the largest peak area in the UV chromatogram.

performed and confirmed such assignments. Successful identification of the "nonspecifically" cleaved peptides led to a high sequence recovery of 99% for both chains. Asp-N peptide 172–174 (Asp-Ser-Lys) in the light chain and 400–401 (Asp-Ser) in the heavy chain were not detected, likely because of their small sizes and hydrophilic nature.

Asp-N peptide mapping suggested similar post-translational modifications in the huN901 heavy chain to those indicated by tryptic mapping. The N-terminal peptide of the heavy chain (HD1; residues 1–61) was found eluting at 133 min owing to the large size and hydrophobic nature of this peptide (Table IV). The mass measurement confirmed transformation of the N-terminal glutamine residue to pyroglutamic acid. The peptide 431–447 was found eluting at 61 min with a mass corresponding to the C-terminal peptide missing the terminal lysine residue (Fig. 10). Peptides linked to oligosaccharides eluted from 92–95 min in the heavy chain mapping (Fig. 9B). These peptides were identified as D12 (residues 281–312) and a subsequence of D12 (residues 295–312; Table IV), indicating that glycosylation occurs at Asn298, consistent with the results from the trypsin digestion.

Interestingly, as shown in Fig. 11A–C, a peptide with one unit mass higher than heavy chain peptide HD13 was found eluting as a shoulder (peak 1) of the HPLC peak of HD13 at 85.9 min (residues 313–356, peak 2), indicating that deamidation had occurred in this peptide, where Asn316 was likely transformed into isoAsp. The aspartate-containing counterpart was further cleaved by Asp-N protease generating a peptide containing residues 316–356 at 78.2 min (Fig. 11D), whose experimental mass had increased by 1 Da over the calculated value, consistent with deamidation at Asn316. These results also agreed with the finding of partial deamidation in the tryptic mapping at Asn316. Similarly, the

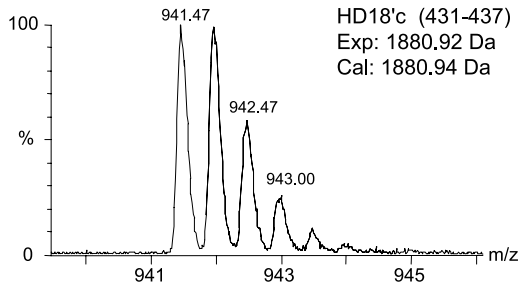

Fig. 10. MS spectrum of huN901 heavy chain C-terminal Asp-N peptide D18′c (431–447).

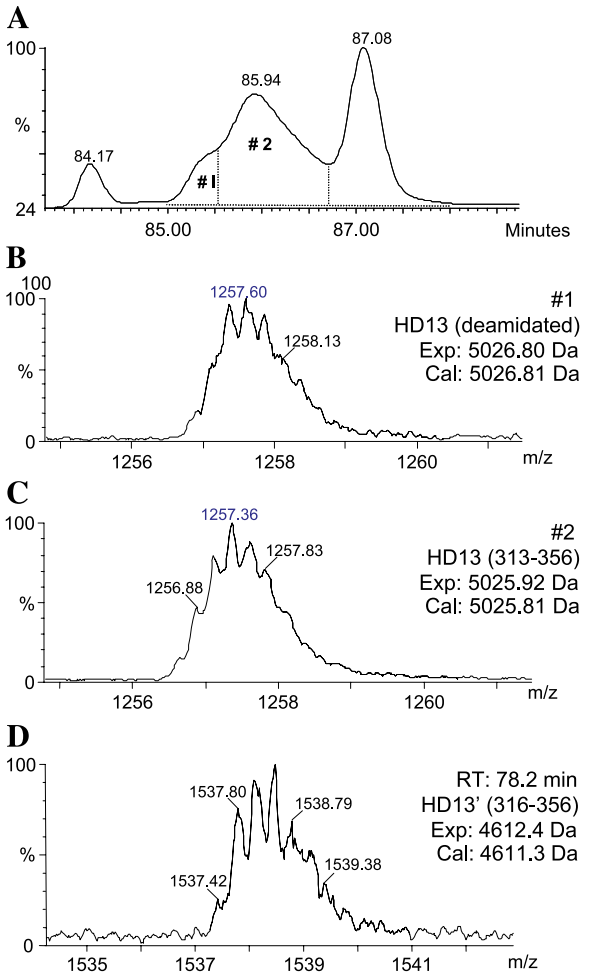

Fig. 11. Enlarged UV chromatogram (A) and MS spectra (B, C, and D) of heavy chain Asp-N protease peptide HD13 and its deamidated products.

other deamidation site identified in tryptic digestion, Asn385, was also confirmed by finding two Asp-N peptides resulting from the further cleavage at Asn385 (data not shown).

DISCUSSION

A structural characterization of huN901 was carried out using both top-down and bottom-up MS approaches. Each approach has its own advantages and may suit different needs. The top-down MS approach serves as a quick method to confirm the protein identity and assess potential post-translational modifications. The other approach of peptide mapping, however, is more time consuming but more structurally informative. It not only identifies the nature of post-translational modifications that likely occur in the protein, but also determines their exact locations. It should be noted that the typical error range of protein mass measurement (+/− 0.01%) limits the identifiable modifications in the first approach to those with relatively large mass differences. The second approach, however, is able to determine modifications with small mass differences, such as the 1-Da increase caused by deamidation. The use of both approaches in this study provided consistent and complementary results, leading to the elucidation of structural details of huN901.

The use of ESI-TOFMS provided several advantages over other types of MS such as quadrupole or magnetic scanning instruments. Both top-down and bottom-up MS approaches can be performed effectively with ESI-TOFMS. On the one hand, the unique capability of TOF mass analyzer of achieving good mass resolution and sensitivity over a broad mass range makes ESI-TOFMS a good method for intact MAb protein analysis. In addition, the high resolution and high mass accuracy of ESI-TOFMS gives reliable peptide mapping results. A mass resolution of over 6000 can be routinely obtained with the LCT ESI-TOFMS used in this study, allowing detection of the charge states of most peptide ions. As a result, peptide masses can be determined with better accuracy than with other low-resolution mass spectrometry methods. Therefore, in most cases, peptides could be assigned according to their measured molecular masses without further confirmation with MS/MS or other techniques such as Edman sequencing or amino acid analysis. Furthermore, the inherent high sensitivity of the TOF mass analyzer also facilitated detection of protein degradation products of low abundances, such as the minor deamidation product (Fig. 7D) in huN901.

One of the difficulties in antibody and other large protein peptide mapping is attributable to the complexity of the digestion mixture containing a large number of peptides. For example, a simulation of a complete trypsin digestion of huN901 generated 65 peptides, without including any modified peptides or peptides resulted from nonspecific cleavages. Even a gradient HPLC separation as long as 2 h is usually not adequate to resolve all peptides of such a mixture. To reduce this complexity and efficiently separate peptides before MS analysis, the reduced and alkylated light and heavy chains of huN901 were separated with denaturing SEC and separately subjected to enzymatic digestion and LC–MS analysis. Thus, the number of peptides was greatly reduced for each analysis and the chances of overlapping peaks in the HPLC separations were accordingly minimized. The use of 3 M GudHCl as the mobile phase of denaturing SEC was found necessary to completely separate the two chains and prevent aggregation.

Post-translational modifications identified in huN901 MAb were also found in other recombinant MAbs. These modifications may or may not affect their biological functions, such as binding affinity and pharmacokenetics. For example, isomerization of an Asp residue in the CDR of an anti-IgE MAb decreased its binding affinity significantly (24). Another example showed that MAb OKT3 still retained 80% activity even when 90% of Asn386 in the heavy chain has undergone deamidation (20). Evaluation of deamidation in a HER2 MAb showed that one deamidation site in the light chain slightly reduced potency, whereas the formation of isoAsp102 in one heavy-chain CDR greatly affected potency (8). The impact of the presence of C-terminal lysine in recombinant MAbs on biological functions, however, are unknown at present (25). Identification of post-translational modifications in huN901 MAb, although none was found in CDRs, serves as a first step to evaluate their possible effects on the function of the MAb.

In summary, the primary structure and post-translational modifications of huN901 were characterized by both top-down and bottom-up MS approaches in this study. Modifications of N-terminal pyroglutamate formation, cleavage of C-terminal lysine, glycosylation, and deamidation were identified in the antibody heavy chain by both protein mass measurement and peptide mapping. No modifications were found in the CDRs of both chains. In the peptide mapping procedure, separation of the light and heavy chains before enzymatic digestion reduced the degree of peak overlapping in HPLC separation and facilitated peptide identification. Both trypsin and Asp-N protease were used in digestion to generate complementary mapping results with complete sequence recovery. The techniques described in this study should be applicable to structural characterization of other large and complex protein pharmaceuticals.

ACKNOWLEDGMENTS

We would like to thank Drs. Alex Lazar and John Thomas for many helpful discussions.

REFERENCES

1. M. A. Roguska, J. T. Pedersen, C. A. Keddy, A. H. Henry, S. J. Searle, J. M. Lambert, V. S. Goldmacher, W. A. Blättler, A. R. Rees, and B. C. Guild. Humanization of murine monoclonal antibodies through variable domain resurfacing. *Proc. Natl. Acad. Sci. USA* **91**:969–973 (1994).
2. M. C. Manning, K. Patel, and R. T. Borchard. Stability of protein pharmaceuticals. *Pharm. Res.* **6**:903–918 (1989).
3. T. J. Ahern and M. C. Manning. *Stability of Protein Pharmaceuticals: Part A, Chemical and Physical Pathways of Protein Degradation*, Plenum, New York, 1992.
4. L. C. Santora, I. S. Krull, and K. Grant. Characterization of recombinant human monoclonal tissue necrosis factor-α antibody using cation-exchange HPLC and capillary isoelectric focusing. *Anal. Biochem.* **275**:98–109 (1999).
5. J. Bongers, J. J. Cummings, M. B. Ebert, M. M. Federici, L. Gledhill, D. Gulati, G. M. Hilliard, B. H. Jones, K. R. Lee, J. Mozdzanowski, M. Naimoli, and S. Burman. Validation of a peptide mapping method for a therapeutic monoclonal antibody: what could we possibly learn about a method we have run 100 times? *J. Pharm. Biomed. Anal.* **21**:1099–1128 (2000).
6. D. A. Lewis, A. W. Guzzetta, W. S. Hancock, and M. Costello. Characterization of humanized anti-TAC, an antibody directed against the interleukin 2 receptor, using electrospray ionization mass spectrometry by direct infusion, LC/MS, and MS/MS. *Anal. Chem.* **66**:585–595 (1994).
7. W. Zhang and M. J. Czupryn. Free sulfhydryl in recombinant monoclonal antibodies. *Biotechnol. Prog.* **18**:509–513 (2002).
8. R. J. Harris, B. Kabakoff, F. D. Macchi, F. J. Shen, M. K. Wong, J. D. Andya, S. J. Shire, N. Bjork, K. Totpal, and A. B. Chen. Identification of multiple sources of charge heterogeneity in a recombinant antibody. *J. Chromatogr., B* **752**:233–245 (2001).
9. L. A. Marzilli, W. Zhang, J. Banas, and J. C. Rouse. Intact characterization of monoclonal antibody charge isoforms using nanoESI Q-TOF MS. *Proceedings of the 50th Conference on Mass Spectrometry and Allied Topics*, Orlando, FL, USA, 2002.
10. F. Cottee, N. Haskins, D. Bryant, C. Eckers, and S. Monte. The use of accurate mass measurement by orthogonal time-of-flight mass spectrometry in pharmaceuticals research. *Eur. J. Mass Spectrom.* **6**:210–224 (2000).
11. K. Zhu, J. Kim, C. Yoo, F. R. Miller, and D. M. Lubman. High sequence coverage of proteins isolated from liquid separations of breast cancer cells using capillary electrophoresis-time-of-flight MS and MALDI-TOF MS mapping. *Anal. Chem.* **75**:6209–6217 (2003).
12. F. Sobott, G. M. G. McCammon, H. Hernandez, and C. V. Robinson. A high-mass Q-TOF for the analysis of protein complexes. *Proceedings of the 50th conference on Mass Spectrometry and Allied Topics*, Orlando, FL, USA, 2002.
13. L. C. Santora, I. S. Krull, and K. Grant. Determination of recombinant monoclonal antibodies and noncovalent antigen INFα trimer using Q-TOF mass spectrometry. *Spectroscopy* **17**:50–57 (2002).
14. T. J. Lynch Jr., J. M. Lambert, F. Coral, J. Shefner, P. Wen, W. A. Blättler, A. R. Collinson, P. D. Ariniello, G. Braman, S. Cook, D. Esseltine, A. Elias, A. Skarin, and J. Ritz. Immunotoxin therapy of small-cell lung cancer: a phase I study of N901-blocked ricin. *J. Clin. Oncol.* **15**:723–734 (1997).
15. M. A. Roguska, J. T. Pedersen, A. H. Henry, S. M. Searle, C. M. Roja, B. Avery, M. Hoffee, S. Cook, J. M. Lambert, W. A. Blättler, A. R. Rees, and B. C. Guild. A comparison of two murine monoclonal antibodies humanized by CDR-grafting and variable domain resurfacing. *Protein Eng.* **9**:895–904 (1996).
16. F. V. Fossella, A. Tolcher, M. Elliott, J. M. Lambert, R. Lu, R. Zinner, C. Lu, Y. Oh, B. Forouzesh, H. McCreary, E. K. Rowinsky, P. Barrington, Y. Miller, and K. Dawson. Phase I trial of the monoclonal antibody conjugate, BB-10901, for relapsed/refractory small cell lung cancer (SCLC) and other neuroendocrine (NE) tumors. *American Society of Clinical Oncology* Annual Meeting, Orlando, FL, USA, 2002.
17. G. D. Roberts, W. P. Johnson, S. Burman, K. R. Anumula, and S. A. Carr. An integrated strategy for structural characterization of the protein and carbohydrate components of monoclonal antibodies: application to anti-respiratory syncytial virus MAb. *Anal. Chem.* **67**:3613–3625 (1995).
18. N. Viseux, X. Hronowski, J. Delaney, and B. Domon. Qualitative and quantitative analysis of the glycosylation pattern of recombinant proteins. *Anal. Chem.* **73**:4755–4762 (2001).
19. J. A. Saba, J. P. Kunkel, D. C. Jan, W. E. Ens, K. G. Standing, M. Butler, J. C. Jamieson, and H. Perreault. A study of immunoglobulin G glycosylation in monoclonal and polyclonal species by electrospray and matrix-assisted laser desorption/ionization mass spectrometry. *Anal. Biochem.* **305**:16–31 (2002).
20. D. J. Kroon, A. Baldwin-Ferro, and P. Lalan. Identification of sites of degradation in a therapeutic monoclonal antibody by peptide mapping. *Pharm. Res.* **9**:1386–1393 (1992).
21. W. Zhang and M. J. Czupryn. Characterization of asparagine deamidation and aspartate isomerization in recombinant human interleukin-11. *Pharm. Res.* **19**:1223–1231 (2002).
22. W. Zhang and M. J. Czupryn. Analysis of isoaspartate in a recombinant monoclonal antibody and its charge isoforms. *J. Pharm. Biomed. Anal.* **30**:1479–1490 (2003).
23. C. Oliyai and R. Borchardt. Chemical pathways of peptide degradation. IV. Pathways, kinetics, and mechanism of degradation of an aspartyl residue in a model hexapeptide. *Pharm. Res.* **10**:95–102 (1993).
24. J. Cacia, R. Keck, L. G. Presta, and J. Frenz. Isomerization of an aspartic acid residue in the complementarity-determining regions of a recombinant antibody to human IgE: identification and effect on binding affinity. *Biochemistry* **35**:1897–1903 (1996).
25. R. J. Harris. Processing of C-terminal lysine and arginine residues of proteins isolated from mammalian cell culture. *J. Chromatogr., A.* **705**:129–134 (1995).